Combining high mass resolution and velocity imaging in a time-of-flight ion-spectrometer using pulsed fields and an electrostatic lens

doi: 10.1063/1.2774823

Combining high mass resolution and velocity imaging in a time-of-flight ion spectrometer using pulsed fields and an electrostatic lens

G. Prümper,[a] H. Fukuzawa, T. Lischke, and K. Ueda
Institute of Multidisciplinary Research for Advanced Materials, Tohoku University, Sendai 980-8577, Japan

(Received 19 June 2007; accepted 31 July 2007; published online 23 August 2007)

We describe a momentum resolving time-of-flight ion mass spectrometer that combines a high mass resolution, a velocity focusing condition for improved momentum resolution, and field-free conditions in the source region for high resolution electron detection. It is used in electron-ion coincidence experiments to record multiple ionic fragments produced in breakup reactions of small to medium sized molecules, such as $F_3SiCH_2CH_2Si(CH_3)_3$. These breakup reactions are caused by soft x rays or intense laser fields. The ion spectrometer uses pulsed extraction fields, an electrostatic lens, and a delay line detector to resolve the position. Additionally, we describe a simple analytical method for calculating the momentum from the measured hit position and the time of flight of the ions. © *2007 American Institute of Physics.* [DOI: 10.1063/1.2774823]

I. INTRODUCTION

Energy-or momentum-resolved electron-ion coincidence techniques have developed rapidly in the last decade: see, for example, papers collected in Ref. 1. One of the breakthroughs in the progress of coincidence techniques has been brought by the development of position-sensitive detectors with multihit capability. Use of such detectors allows one to register three-dimensional (3D) momenta k for more than one charged particle.

The best-known k-revolved electron-ion coincidence technique is the one often called cold target recoil ion momentum spectroscopy[2] (COLTRIMS) or reaction microscope.[3] In this technique, all electrons and ions produced by a single multiple ionization event are projected by a static electric field onto two position-sensitive detectors placed on opposite sides. This method, which has high collection efficiency and thus high coincidence rates, is extremely powerful for studying atomic or diatomic double ionization where two electrons with one ion or two can be detected in coincidence and thus kinematically complete information can be extracted.

The experimental requirements for the ionization of polyatomic molecules are more demanding. First the number of different fragments is much larger and it is necessary to avoid overlap in the mass spectrum for fragments that differ only by 1 amu. Second, the data evaluation procedure cannot make use of momentum conservation, as usually neutral fragments are emitted. Nevertheless for a detailed understanding of these reactions, the coincident measurement of at least one electron and all occurring ionic fragments including their momenta is very helpful. However, one faces the difficulty to use COLTRIMS or a reaction microscope for such study because of restrictions arising from the fact that the same static electric field is used to extract both electrons and ions. So either one has to compromise on electron energy resolution or ion mass resolution.

We have developed an electron-ion coincidence setup for studying breakup reactions of polyatomic molecules after the irradiation with soft x rays[4–10] or by strong optical fields in intense femtosecond laser pulses.[11] In this article we will describe the ion time-of-flight (TOF) spectrometer. Further details of the coincidence setup[4,5] and the data evaluation procedure[12] are reported elsewhere.

Our ion TOF spectrometer has two key features, i.e., *pulsed fields* (see, for example, Refs. 13–15) and *velocity imaging*.[16–20]

To obtain velocity imaging of our ion spectrometer we have mounted a lens inside the drift tube, just after the entrance grid of the drift tube. Similar designs have been reported by Lebech *et al.*[21] and later by Hosaka *et al.*[22] However, a completely new design was necessary due to the use of pulsed fields and to meet the requirements for high mass and momentum resolution. Before describing the detailed design of the spectrometer, we briefly address the two key features pulsed fields and velocity imaging as part of an extended introduction.

A. Pulsed fields

The ions that are created in the interaction region can be extracted using electric fields. If the fields are chosen properly, the hit position on the detector and the hit time allow a reconstruction of the ion momentum. The ions can be extracted by using static or pulsed electric fields. The use of static fields is much easier and has many advantages. Simple power supplies can be used, there is no time delay between the ionization and the ion extraction, therefore all ions can be collected from the source region, and there is no problem due to electronic noise produced by fast switching of the pulsed extraction fields. Especially in short time-of-flight spectrometers such noise can overlap with the arrival time of light

[a]Electronic mail: pruemper@tagen.tohoku.ac.jp

ions, and therefore an electronic gate cannot be used to suppress the noise signal.

However, there are intrinsic disadvantages of using static fields, if the kinetic energy of electrons has to be analyzed in a coincidence experiment. Generally the kinetic energy of the electrons and the one of the ions are very different and additional magnetic fields have to be used to get a good compromise for the acceptance angles and energy resolutions for the electrons and ions. Without using a magnetic field one typically has an acceptance angle for electrons of ±20° in the forward and backward emission directions of the electrons along the spectrometer axis. Fast electrons emitted perpendicular to the spectrometer axis do not hit the detector. Simply using a higher electric extraction field would result in a loss of energy resolution.

Another problem cannot be solved using static fields only: if the electrons come from a region that is not field-free, they get an additional spread of the kinetic energy due to the size of the source volume. Typical values are 10 V/mm for the extraction field and 0.1 mm for the source diameter. So the additional energy spread due to the potential variation in the source volume is 1 eV, which is by far too much for many spectroscopic studies. This problem can be overcome by the use of pulsed fields. The idea is very simple. The ionization takes place in a field-free source region. As the electrons are much lighter than the ions, they reach the detector after typically some 100 ns, depending on the kinetic energy on their way through the spectrometer. This measurement can be performed with the standard techniques of high resolution electron spectroscopy, such as time-of-flight spectrometers or dispersive spectrometers. For the latter method the time of flight of the electrons depends on the pass energy used. Neglecting the time of flight through the lens of the electron spectrometer, the electrons need about 140 ns to pass the half spheres with a mean radius of 200 mm with a pass energy of 50 eV. For a pass energy of 500 eV this time reduces to about 45 ns. During the time of flight of the electron the ions travel only a few millimeters at most. A strong electric extraction field is applied after the electron is detected, and the ions are projected on the position-sensitive detector.

B. Velocity imaging

In order to obtain a good mass and momentum resolution, ion optics are very helpful to demagnify the image of the source region on the detector. In this way the hit position on the detector is a measure of the transversal momentum only and does not depend on the starting position of the ion. Another benefit of the lens is that it increases the kinetic energy range in which the instrument has a 4π sr collection efficiency. So velocity focusing gives not only a better momentum resolution but also a larger momentum range. Therefore we combined the two methods: a pulsed field in the first part of the spectrometer and an electrostatic lens further downstream inside the drift tube. One problem with the use of lenses is that the calculation of the initial ion momentum from the measured time of flight and detector hit position becomes nontrivial. One can no longer use simple analytical formulas describing, e.g., trajectories in homogeneous electric fields but one is forced to use numerical calculations of the trajectories. However, it turns out that in some cases the effect of the lens can be modeled easily, by a small modification in the analytical treatment.

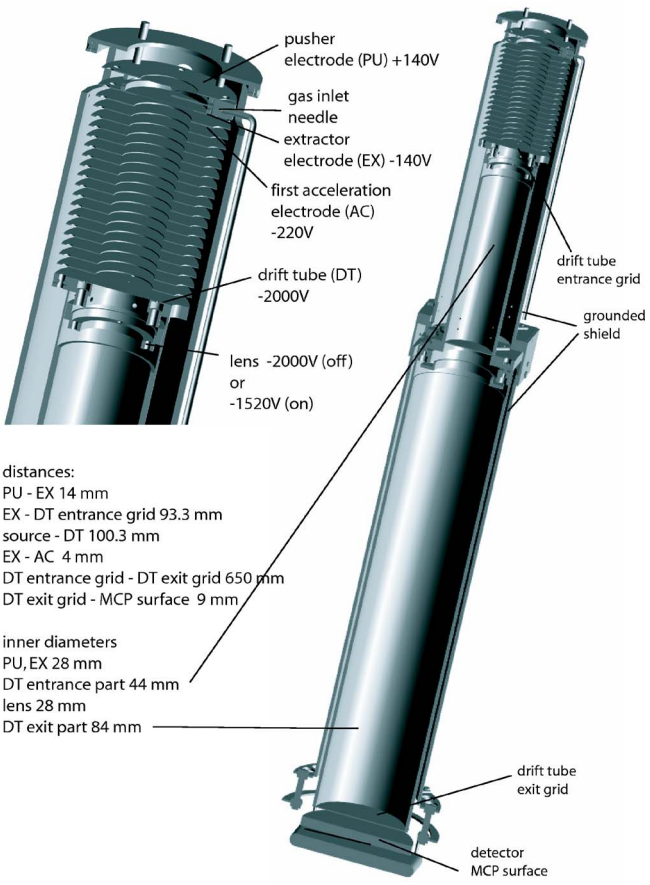

FIG. 1. The ion time-of-flight spectrometer with typical operation voltages.

II. DESIGN OF THE SPECTROMETER

The ion spectrometer is shown in Fig. 1. It consists of two electrodes for the ion extraction called pusher and extractor and a 650 mm long electrode, called the drift tube. All electrodes are made from simple flat plates with holes and tubes. Only nonmagnetic materials may be used, as this instrument is to be used in an experiment involving electron energy analysis. Because the source size is small in the direction of the spectrometer axis in our experiments, we decided to violate the space focusing condition in that direction[23] in favor of an increased mass and momentum resolution and momentum range. In the region between the extractor and the drift tube there is an acceleration region consisting of several ring shaped electrodes, connected by resistors. In order to get homogeneous fields and to avoid field penetration of the drift tube voltage to the source region the holes of the pusher and extractor electrodes are covered with high transmission (80%) copper grids. The electric field in the acceleration region between the extractor and the drift tube is the same as the field between the pusher and extractor electrode when the high voltage (HV) pulse is applied. The purpose of the grid on the extractor electrode is merely to

avoid field penetration into the source region before the HV pulse is turned on. The overall length of the system is about 750 mm. The usable active diameter of the detector is about 75 mm. The pulsed extraction field is applied symmetrically (typically ±140 V) to the pusher and extractor electrodes. It is applied about 400 ns after the ionization of the molecules by a light pulse, coming from a laser or a synchrotron radiation (SR) source. In case of the SR the trigger for the electric field comes from an electron detector; therefore, the total delay is the electron time of flight through the electron spectrometer, i.e., some 100 ns, plus an electronic delay of about 150 ns. In laser based experiments the delay is similar. In this case one typically records much slower electrons with kinetic energies down to 0.5 eV. Therefore the insertion delay is about 400 ns in both types of experiments. The use of symmetric pulses at the pusher and extractor simplifies the mechanical design, because the source region can be kept at ground potential. After leaving the extraction region, the ions are accelerated towards the drift tube. Typically the static voltage for the drift tube is −2000 V. Energetic ionic fragments may hit the ion detector far off axis, so a large position resolving delay line detector (DLD) with 75 mm active diameter is used. The lens for velocity focusing is mounted inside the drift tube. If it is set to the same voltage as the drift tube, the inside of the drift tube is field-free and the trajectories can be calculated using homogeneous electric fields. We made use of this feature in a reference measurement to compare it with the more complicated case using the lens in the velocity imaging mode.

III. METHOD FOR MOMENTUM RECONSTRUCTION

The motion of an ion inside the spectrometer has two phases. The field-free phase, before the voltage is applied and the extraction phase, when the HV pulse is applied. During the field-free phase the ions move along straight lines with their initial speed. When the HV pulse is applied the second phase starts. Then the ion flies through the acceleration region of constant electric field before entering the field-free drift tube. All phases can be described using simple analytical formulas leading to a relatively simple relation between the components of the initial momentum p_x, p_y, p_z and the time of flight T and the detector hit radius r. The use of the lens leads to deviations from this model.

The optimum voltage for the velocity imaging, i.e., the best demagnification of the source volume, was determined empirically in a SR experiment using N_2 as target molecules. The illumination of the detector by the doubly charged parent molecules was measured for various voltages of the lens. The optimum value for the lens voltage was determined as −1520 V, reducing the image of the approximately 20 mm long source region to a spot smaller than 5 mm in diameter. This result is consistent with the calculation of the trajectories using the SIMION program.[24] These simulations showed that using this voltage, the source is focused to a spot smaller than 1 mm in diameter. The remaining discrepancy of the simulation results and the measured spot size is most likely due to the use of grids,[20] which were simulated in a very idealized way.

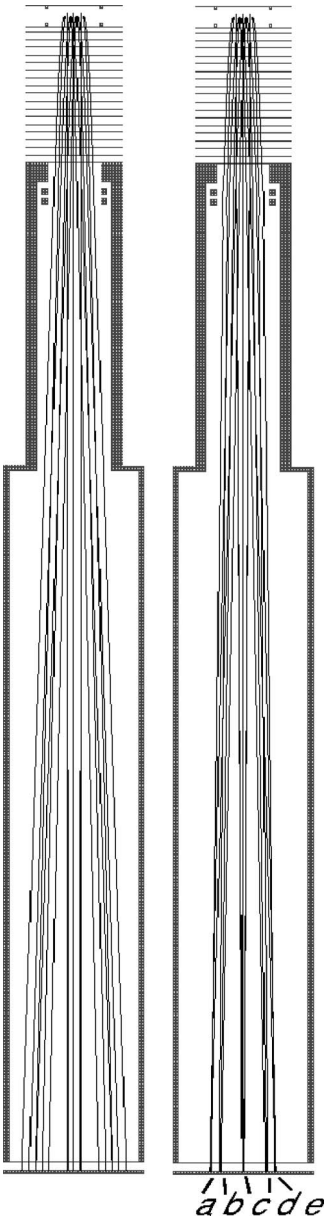

FIG. 2. Simulation results. The left half of the figure shows the simulation results with the lens turned off, whereas the right half shows the result for the lens turned on. Each half of the figure includes in total 24 trajectories for N^+ ions with kinetic energies of 1 and 2 eV starting from three different points horizontally separated by 3 mm. They fly in the directions up, down, left, and right. All trajectories start after 400 ns of free flight. One can see that in the right figure the trajectories cluster at five hit points on the detector: (a) the 2 eV electrons emitted to the left, (b) 1 eV electrons emitted to the left, (c) electron emitted up and down, (d) 1 eV electrons emitted to the right, and (e) 2 eV electrons emitted to the right. The velocity focusing and demagnification are clearly visible.

Therefore we conclude that once the lens is used, the starting position of the ion does only affect the time of flight, but not the hit position of the detector. This is a crucial point in developing a simple method for the calculation of the momentum when the lens is used. To confirm this behavior we compared the calculated illumination of the detector for 0.1, 1, 2, and 3 eV ions for two cases: (A) no insertion delay, i.e., static electric fields and (B) the HV pulse applied, after the ions moved 5 mm away from the source point. We did not find any significant change in the detector hit radius. This

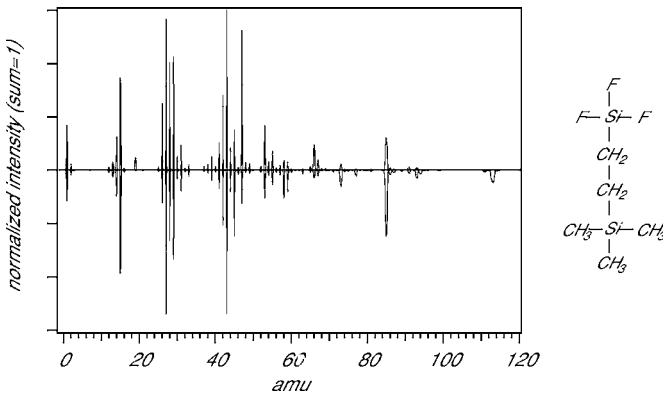

FIG. 3. Example for the mass resolution achieved in an electron ion coincidence experiment. $F_3SiCH_2CH_2Si(CH_3)_3$ was ionized using 400 eV soft x-ray photons leading to the ejection of a Si $2p$ core electron (Ref. 10). The Si $2p$ electrons originating from the F side and the CH_3 side were distinguished by the kinetic energy of the electron. The corresponding ion time-of-flight spectra are plotted in the positive and negative directions.

result is consistent with the very idea of velocity focusing: the detector hit position should depend on the initial momentum but not on the position when the HV pulse is applied.

Next we calculated the effect of the lens on the detector illumination. We assumed a point source and a dc voltage applied to pusher and extractor (zero insertion delay) and studied the effect of the lens on the illumination of the detector, i.e., we compared the detector illumination for the lens switched on and off. For the energies 0.5, 1, 2, 3, and 4 eV we found a constant demagnification factor of 0.72.

Based on these results we assume that the following simple recipe is a good approximation for modeling the relation between momentum p_x, p_y, p_z, and the measured values for time of flight T and detector hit position (radius) r.

(1) For a known value of the insertion delay d, the voltages, and the dimensions of the spectrometer the time of flight T of ion with mass m, charge c, and momentum p_z is calculated assuming homogeneous electric fields without the lens effect. p_z is the momentum component along the spectrometer axis. T does depend on p_z, but T does not depend on p_x and p_y. T is counted from the moment of the light pulse, i.e., it contains the insertion delay d.
(2) The calculated T is corrected by an empirical factor f_c that is close to 1, which is known from the empirical mass scale determined from the time of flight of two ions with different masses, i.e., from two peaks in the TOF spectrum. $T_c = f_c(T-d)+d$. This factor is valid for the whole mass range. It is universal for all masses, because independent of the spectrometer geometry and the voltages applied the time of flight for nonenergetic ions is always proportional to the square root of the mass to charge ratio.
(3) The hit radius r is calculated as the product of T_c and the transversal velocity of the ion $v_t = p_t/m$, where p_t is assumed not to change during the flight through the spectrometer. It should be noted that r does not include the effect of the motion of the ion before the HV pulse is applied. This corresponds to the velocity imaging condition. Finally, r is multiplied by 0.72.

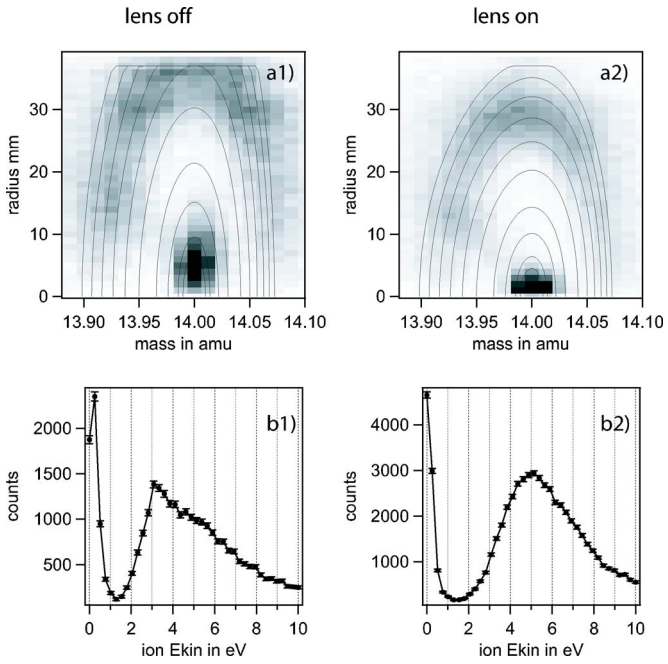

FIG. 4. Example for the momentum resolution achieved in an electron ion coincidence experiment. N_2 was ionized using 792 eV soft x-ray photons. The N $1s$ photoelectrons were used to trigger the ion extraction. The energetic N^+ and thermal N_2^{++} ions were detected. The time of flight is converted to mass scale. We compare the two operation modes. On the left part of the figure the velocity imaging lens is off, whereas on the right part it is off. (The two segments of the lens were put to the same voltage.) The use of the lens leads to an improvement of the momentum resolution and an extension of the kinetic energy range with 4π sr collection efficiency. The concentric curves in the upper two panels belong to the calculated trajectories of N^+ ion with kinetic energies: 0.1, 0.2, 0.5, 1, 2, 3, 4, 5, 6, and 7 eV (counting from the center to the outside). See text for details. The intensity distribution is mainly given by trivial geometrical effects. There is less chance to hit a 5 mm radius than to hit a 20 mm radius because large hit radii correspond to a larger solid angle interval.

As this recipe only involves analytical formulas it is easily inverted and can conveniently be used to calculate p_t and p_z from the measured values of T and r.

Figure 2 shows example results of the simulation.

IV. PERFORMANCE TESTS

A. Mass resolution

As expected from the simulation and confirmed in our test, the mass resolution does not change significantly when the lens is used. Only the mass scale, i.e., the relation between T and the mass for nonenergetic fragments, is slightly modified when the lens is used. The effect of this can easily be included in the scaling factor f_c described above. The obtainable mass resolution was amply demonstrated in an earlier experiment, not using the velocity focusing mode:[10] the mass spectra of $F_3SiCH_2CH_2Si(CH_3)_3$ irradiated by 400 eV soft x-ray photons leading to Si $2p$ core ionization. The Si $2p$ photoelectrons originating from the F side and the CH_3 side were distinguished by their kinetic energies. The corresponding ion mass spectra are plotted in the positive and negative directions in Fig. 3. For details, see Ref. 10.

B. Momentum resolution

In order to measure the momentum resolution and to verify the recipe to reconstruct the momentum from the TOF and hit radius, we performed two measurements. One with the lens set to −2000 V (off) and one with the lens set to −1520 V (on). The target gas was N_2 ionized using 792 eV soft x-ray photons. The detected N 1*s* photoelectrons were used to trigger the ion extraction. Energetic N^+ ions and thermal N_2^{++} ions were detected.

Figure 4 shows the result in four panels. Panels (a1) and (a2) are intensity plots as a function of the TOF and the detector hit radius *r*. The TOF has been converted to mass in amu. One can see two contributions: a small center spot that belongs to thermal N_2^{++} ions mainly hitting the center of the detector and a half ring of energetic N^+ ions hitting the detector at large radii for time-of-flight values corresponding to the middle of the peak and the center of the detector for TOF values corresponding to ion emission parallel and antiparallel to the spectrometer axis. The solid concentric curves in the upper two panels belong to the calculated trajectories of N^+ ion with kinetic energies: 0.1, 0.2, 0.5, 1, 2, 3, 4, 5, 6, and 7 eV (counting from the center to the outside). Along one curve the emission direction of the ion was varied from parallel to the spectrometer axis to perpendicular to antiparallel to spectrometer axis. One can easily see that according to this calculation, in the measurement with the lens switched off, the kinetic energy range with 4π sr detection efficiency is limited to 3 eV, while it goes up to about 6.5 eV when the lens is used. This is because of two mechanisms: first the velocity focusing removes the effect of the source size and the spread of the ions during the insertion delay and second the demagnification factor of 0.72 further contracts the rings. The lower two panels (b1) and (b2) are the corresponding kinetic energy spectra of the ions. One can see that the 0 eV peak of the N_2^{++} ions becomes sharper, due to the smaller image of the source region on the detector. Further one can see that the true maximum of the distribution at about 5 eV is only visible when the lens is used. Without the lens, the distribution above 3 eV suffers from the reduced collection efficiency.

V. DISCUSSION

We have shown that an instrument using pulsed extraction fields and a lens for velocity imaging can be used for the determination of the ion momentum while maintaining a high mass resolution for target molecules of a mass of 100–200 amu. This technique is a major improvement in experiments involving the coincident detection of electrons and the detection of multiple ionic fragments including their momentum.

ACKNOWLEDGMENTS

The experiment was carried out with the approval of JASRI and was partly supported by the Japan Society of the Promotion of Science (JSPS) in the form of Grants-in-Aid for Scientific Research. The staff of SPring-8 are greatly acknowledged for providing an excellent experimental facility.

[1] K. Ueda, J. Electron Spectrosc. Relat. Phenom. **141**, 73 (2004).
[2] R. Dörner, V. Mergel, O. Jagutzki, L. Spielberger, J. Ullrich, R. Moshammer, and H. Schmidt-Böcking, Phys. Rep. **330**, 95 (2000).
[3] J. Ullrich, R. Moshammer, A. Dorn, R. Dörner, L. P. H. Schmidt, and H. Schmidt-Böcking, Rep. Prog. Phys. **66**, 1463 (2003).
[4] G. Prümper, Y. Tamenori, A. D. Fanis, U. Hergenhahn, M. Kitajima, M. Hoshino, H. Tanaka, and K. Ueda, J. Phys. B **38**, 1 (2005).
[5] G. Prümper, K. Ueda, U. Hergenhahn, A. D. Fanis, Y. Tamenori, M. Kitajima, M. Hoshino, and H. Tanaka, J. Electron Spectrosc. Relat. Phenom. **144–146**, 227 (2005).
[6] X. J. Liu *et al.*, Phys. Rev. A **72**, 042704 (2005).
[7] G. Prümper *et al.*, Phys. Rev. A **71**, 052704 (2005).
[8] H. Fukuzawa, G. Prümper, S. Nagaoka, T. Ibuki, Y. Tamenori, J. Harries, X. J. Liu, and K. Ueda, Chem. Phys. Lett. **431**, 253 (2006).
[9] H. Fukuzawa *et al.*, Chem. Phys. Lett. **436**, 51 (2007).
[10] S. Nagaoka *et al.*, Phys. Rev. A **75**, 020502 (2007).
[11] T. Hatamoto, G. Prümper, M. Okunishi, D. Mathur, and K. Ueda, Phys. Rev. A **75**, 061402 (2007).
[12] G. Prümper and K. Ueda, Nucl. Instrum. Methods Phys. Res. A **574**, 350 (2007).
[13] C. Miron, M. Simon, N. Leclercq, D. L. Hansen, and P. Morin, Phys. Rev. Lett. **81**, 4104 (1998).
[14] O. Kugeler, G. Prümper, R. Hentges, J. Viefhaus, D. Rolles, U. Becker, S. Marburger, and U. Hergenhahn, Phys. Rev. Lett. **93**, 033002 (2004).
[15] D. Céolin, C. Miron, M. Simon, and P. Morin, J. Electron Spectrosc. Relat. Phenom. **144**, 171 (2004).
[16] D. H. Parker and A. T. J. B. Eppink, J. Chem. Phys. **107**, 2357 (1997).
[17] M. Takahashi, J. P. Cave, and J. H. D. Eland, Rev. Sci. Instrum. **71**, 1337 (2000).
[18] G. A. Garcia, L. Nahon, C. J. Harding, E. A. Mikajlo, and I. Powis, Rev. Sci. Instrum. **76**, 053302 (2005).
[19] A. I. Chichinin, T. Einfeld, C. Maul, and K. H. Gericke, Rev. Sci. Instrum. **73**, 1856 (2002).
[20] A. T. J. B. Eppink and D. H. Parker, Rev. Sci. Instrum. **68**, 3477 (1997).
[21] M. Lebech, J. Houver, and D. Dowek, Rev. Sci. Instrum. **73**, 1865 (2002).
[22] K. Hosaka, J. Adachi, A. Golovin, M. Takahashi, N. Watanabe, and A. Yagishita, Jpn. J. Appl. Phys., Part 1 **45**, 1841 (2005).
[23] W. C. Wiley and I. H. McLaren, Rev. Sci. Instrum. **26**, 1150 (1955).
[24] D. A. Dahl, J. E. Delmore, and A. D. Appelhans, Rev. Sci. Instrum. **61**, 607 (1990).